■ DNA Groove Binding

Sensing of Double-Stranded DNA/RNA Secondary Structures by Water Soluble Homochiral Perylene Bisimide Dyes

Jana Gershberg,[a] Marijana Radić Stojković,[b] Marko Škugor,[b] Sanja Tomić,[b] Thomas H. Rehm,[a] Stefanie Rehm,[a] Chantu R. Saha-Möller,[a] Ivo Piantanida,*[b] and Frank Würthner*[a]

Abstract: A broad series of homochiral perylene bisimide (PBI) dyes were synthesized that are appended with amino acids and cationic side chains at the imide positions. Self-assembly behavior of these ionic PBIs has been studied in aqueous media by UV/Vis spectroscopy, revealing formation of excitonically coupled H-type aggregates. The interactions of these ionic PBIs with different ds-DNA and ds-RNA have been explored by thermal denaturation, fluorimetric titration and circular dichroism (CD) experiments. These PBIs strongly stabilized ds-DNA/RNA against thermal denaturation as revealed by high melting temperatures of the formed PBI/polynucleotide complexes. Fluorimetric titrations showed that these PBIs bind to ds-DNA/RNA with high binding con-

stants depending on the number of the positive charges in the side chains. Thus, spermine-containing PBIs with six positive charges each showed higher binding constants ($\log K_s =$ 9.2–9.8) than their dioxa analogues ($\log K_s = 6.5$–7.9) having two positive charges each. Induced circular dichroism (ICD) of PBI assemblies created within DNA/RNA grooves was observed. These ICD profiles are strongly dependent on the steric demand of the chiral substituents of the amino acid units and the secondary structure of the DNA or RNA. The observed ICD effects can be explained by non-covalent binding of excitonically coupled PBI dimer aggregates into the minor groove of DNA and major groove of RNA which is further supported by molecular modeling studies.

Introduction

Nucleic acids are most important biomolecules as they code the information of life. Thus, small molecules targeting deoxyribonucleic acid (DNA) and ribonucleic acid (RNA) have attracted significant scientific interest due to medicinal, biochemical and biological implications of such molecular recognition events.[1] For instance, sequence specific detection of double-stranded (ds)-DNA and (ds)-RNA by molecular recognition has become increasingly more valuable as diagnostic tool in molecular biology and medicine.[2] Non-covalent recognition of DNA/RNA by small molecules very often relies on single dominant binding mode such as intercalation, groove binding, or electrostatic sugar-phosphate backbone binding.[3] Only in the last decade small molecules combining two or more dominant non-cova-

lent binding modes have been studied to a larger extent,[3] aiming for new compounds to be able to selectively report on structural differences of DNA and RNA secondary structure. In the recent years, researchers have focused attention on molecules with extended π-cores such as pyrene[4] and perylene[5] derivatives.[6] However, only recently interaction of perylene bisimide (PBI) dyes with DNA and RNA have gained appreciable attention. PBI dyes have been covalently attached to DNA to create DNA conjugates, which self-assemble into duplex and triplex structures by π–π-interactions of PBI molecules.[7] Moreover, PBIs have been studied for selective non-covalent interactions with G-quadruplexes.[8] However, only limited information is available on non-covalent interactions of PBIs with other DNA and RNA structures, like triple helices or specific double-stranded structures.[5,9] Even there studies were often performed as parallel experiments to those with G-quadruplexes.[10] Investigations of PBI-DNA conjugates have shown that stacked PBI molecules within the DNA scaffold give specific induced circular dichroism (ICD) profiles, which are strongly dependent on the freedom of adjustment of PBI molecules in the DNA.[11] This finding suggests that PBI dyes can be used as sensitive probes for the chiral environment of polynucleotides and as non-covalently interacting sensors for various DNA and RNA structures.

In the last decade, Piantanida et al. have been particularly interested in small molecules able to bind efficiently via non-covalent interactions to the most of naturally occurring ds-DNA/RNA as well as to report different signals for each of the most

[a] J. Gershberg, Dr. T. H. Rehm, S. Rehm, Dr. C. R. Saha-Möller, Prof. Dr. F. Würthner
Universität Würzburg, Institut für Organische Chemie and Center for Nanosystems Chemistry
Am Hubland, 97074 Würzburg (Germany)
Fax: (+49) 931-31-84756
E-mail: wuerthner@chemie.uni-wuerzburg.de

[b] Dr. M. Radić Stojković, M. Škugor, Dr. S. Tomić, Dr. I. Piantanida
Division of Organic Chemistry & Biochemistry, Division of Physical Chemistry, Ruđer Bošković Institute
P. O. Box 180, 10002 Zagreb (Croatia)
E-mail: Ivo.Piantanida@irb.hr

🖳 Supporting information for this article is available on the WWW under http://dx.doi.org/10.1002/chem.201500184.

common secondary structures of ds-DNA and RNA by sensitive and biologically applicable methods (e.g., UV/Vis, CD, fluorescence, surface-enhanced Raman spectroscopy).[12] The development of such single-molecule sensors with several properties could replace the necessity of multiple dyes each being specific for one particular DNA or RNA target. The signal selectivity could be achieved by the fine tuning of the interaction of chromophores with secondary structures of polynucleotides which include the introduction of sterically demanding or binding modulating substituents attached to the dye.[12] In this regard, one of the most effective approaches seems to be the variation of selectivity-controlling substituents, which are closely and rigidly attached to the chromophore.

During the last decade, self-assembly of a huge variety of PBI dyes have been investigated and their aggregates have found various applications as (opto)electronic materials.[13] As PBI dyes possess a hydrophobic extended π-core, a particular challenge being the exploration of the aggregation properties of PBI dyes in water which is, however, required for the application of these dyes in biological systems.[14] Beside other approaches, including ionic self-assembly,[14e,d] the attachment of polyamine chains at the imide positions of PBIs provides the necessary solubility of core-planar PBIs in water which make them interesting for the investigation of interactions with biomacromolecules such as DNA.[15] Recently, we have communicated the first examples of spermine-functionalized homochiral PBIs with unique properties such as strong thermal stabilization and high binding affinity towards ds-DNA and RNA.[16]

Here we present our comprehensive studies on the interaction of PBI dyes with a broad variety of polynucleotides by applying a broad new series of homochiral PBIs **(N)**-L- and **(N)**-D-**Phe-PBI**, **(O)**-L- and **(O)**-D-**Ala-PBI** and **(O)**-L- and **(O)**-D-**Phe-PBI**. These PBIs are appended with amino acids possessing substituents of varied sterical demand at the chirality centers and incorporate spermine or 4,9-dioxa-1,12-dodecanediamine side chains at the imide positions (Scheme 1). For the purpose of comparison, we have included in this study the achiral reference compound **(N)-Gly-PBI**[15b] and the previously reported compounds **(N)**-L- and **(N)**-D-**Ala-PBI**.[16] We have investigated the spectroscopic response of the PBIs for structurally different double-stranded DNA and RNA under biologically relevant conditions. For these studies, we have chosen synthetic polynucleotides instead of short oligonucleotides because the latter are not suitable for our investigations due to the "capping" binding of PBIs at the exterior side of alternating base-pairs which would strongly compete with the few binding sites along the double strands of oligonucleotides.[8,17] In contrast, polynucleotides consisting of more than 100 base pairs will assure large excess of binding sites along the double helix, thus the "capping" effect should be negligible. Our detailed thermal denaturation experiments, fluorimetric titrations and CD spectroscopic measurements corroborate strong interactions of the homochiral ionic PBIs with the employed polynucleotides and the formation of excitonically coupled dimer aggregates in the grooves of the ds-DNA/RNA. The binding properties of these PBIs with ds-DNA/RNA are found to be dependent on the number of the positive charges, chirality and

sterical hindrance of the PBIs. Thus, a structure-property relationship could be established.

Results and Discussion

Synthesis

A series of symmetric, homochiral perylene bisimides (denoted as **(N)**-L- and **(N)**-D-**Ala-PBI**, **(N)**-L- and **(N)**-D-**Phe-PBI**, **(O)**-L- and **(O)**-D-**Ala-PBI** and **(O)**-L- and **(O)**-D-**Phe-PBI**) that are appended with α-amino acid derivatives as imide substituents, bearing spermine or its dioxa analogue as side chains, were synthesized from commercially available perylene-3,4:9,10-tetracarboxylic bisanhydride (PBA) in three steps according to the route outlined in Scheme 1. The reaction of PBA with homochiral (L- or D-enantiomer) alanine or phenylalanine in imidazole afforded the corresponding amino acid functionalized symmetrical PBIs L-[18] or D-**Ala-PBI** and L- or D-**Phe-PBI** in excellent yields. The successive amidation of the PBI-appended dicarboxylic acids with threefold Boc-protected spermine **Boc-(N)**[19] using the activation reagents dicyclohexylcarbodimide (DCC) and hydroxylbenzotriazole (HOBt) in DMF led to the spermine-bearing PBI derivatives **Boc-(N)**-L- or **Boc-(N)**-D-**Ala-PBI** and **Boc-(N)**-L- or **Boc-(N)**-D-**Phe-PBI** in 29 to 72% yield. Deprotection of the Boc-groups with trifluoroacetic acid (TFA) afforded the desired products **(N)**-L- or **(N)**-D-**Ala-PBI** and **(N)**-L- or **(N)**-D-**Phe-PBI** as trifluoroacetic salts in quantitative yields, which were then lyophilized from water to obtain them in pure form. For the amidation of the dicarboxylic acids with Boc-protected 4,9-dioxa-1,12-dodecanediamine **Boc-(O)**,[20] however, the activation reagents N,N-diisopropylethylamine (DIPEA) and O-(7-azabenzotriazol-1-yl)-N,N,N′,N′-tetramethyluroniumhexafluorophosphate (HATU), instead of DCC and HOBt were required. The deprotection of Boc-groups in the resulted **Boc-(O)**-L- or **Boc-(O)**-D-**Ala-PBI** and **Boc-(O)**-L- or **Boc-(O)**-D-**Phe-PBI** with TFA afforded the products **(O)**-L- or **(O)**-D-**Ala-PBI** and **(O)**-L- or **(O)**-D-**Phe-PBI** in 84 to 97% yield, which were subsequently purified by lyophilization from water.

The alanine-functionalized compounds **(N)**-L- and **(N)**-D-**Ala-PBI** have previously been reported in our communication.[16] The reference achiral compound **(N)-Gly-PBI** was prepared according to the literature.[15b] All the new compounds were characterized by ^{1}H NMR spectroscopy, high-resolution mass spectrometry and, where possible, also by elemental analysis. The details of the synthesis and characterization data of the new compounds are given in the Supporting Information.

UV/Vis spectroscopic studies of homochiral PBIs

To ascertain the appropriate conditions for the investigation of interactions of these homochiral PBIs with double-stranded (ds)-polynucleotides by different spectroscopic methods such as UV/Vis, fluorescence and circular dichroism (CD) spectroscopy, we have initially performed concentration-dependant UV/Vis studies of these PBIs in water and DMSO (Figure 1 and S1 in Supporting Information). As a representative example of the spermine-containing PBIs (denoted as **(N)**-series), the concen-
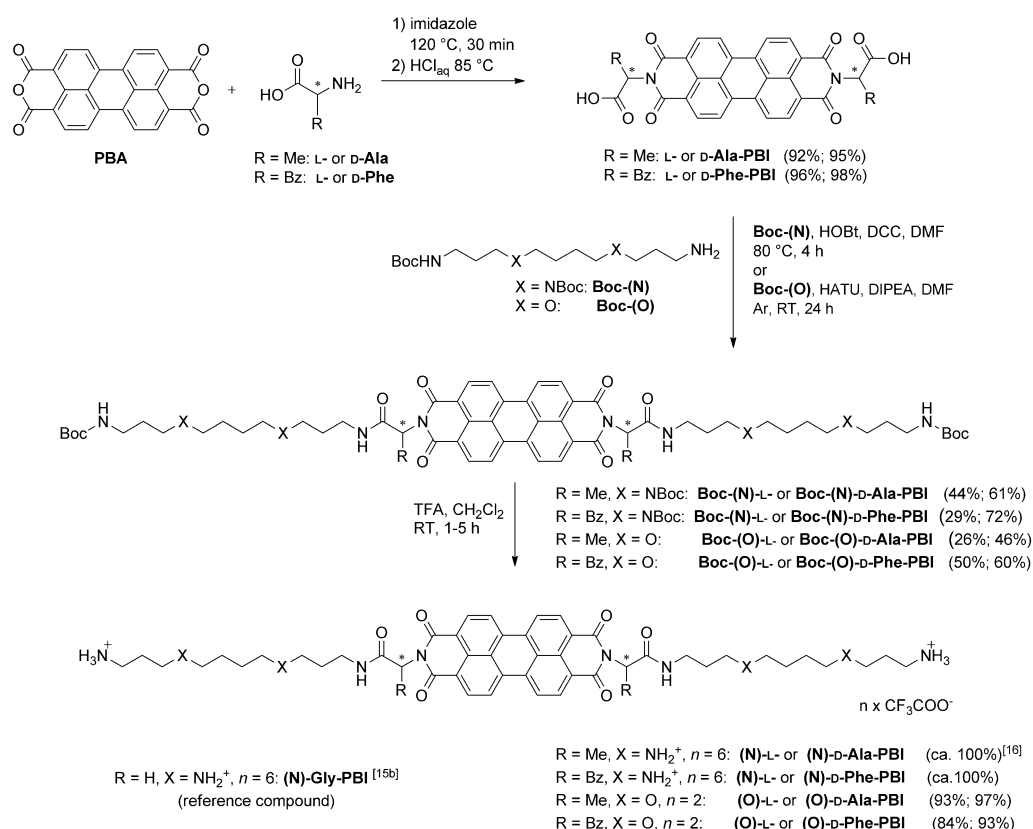
Scheme 1. Synthetic route to amino acid appended homochiral perylene bisimide dyes. Please note that both chirality centers of each of these homochiral PBIs have identical conformation, that is, either L,L or D,D. For simplicity and easier comparison they are denoted as L- and D-enantiomer.

tration-dependent absorption spectra of **(N)-L-Phe-PBI** in pure water are displayed in Figure 1a. At a low concentration of 5×10^{-6} M, this dye exhibits for PBI monomers typical vibronically resolved spectrum with maxima at 537, 500 and 467 nm. With increasing concentration up to 5×10^{-3} M the intensities of monomer bands decreased with concomitant appearance of a strongly hypsochromically shifted band at 508 nm and a slightly red-shifted band at 546 nm, indicating the formation of aggregates with H-type excitonic coupling.[21] Identical concentration-dependent spectral changes were observed for the corresponding D-enantiomer in water (spectra not shown). The concentration-dependent absorption properties of these phenylalanine-functionalized PBIs resemble those of the alanine analogues **(N)-L-** and **(N)-D-Ala-PBI**.[16] Since for the latter dimer formation, and no further growth to extended aggregates due to electrostatic repulsion of positive charges, was confirmed in the given concentration range, similar behavior can be assumed for the phenylalanine derivatives **(N)-L-** and **(N)-D-Phe-PBI**. In contrast to spermine-bearing PBIs (the **(N)**-series), the absorption spectra of their dioxa analogues **(O)-L-** and **(O)-D-Ala-PBI**, and **(O)-L-** and **(O)-D-Phe-PBI** revealed over the whole concentration range from 5×10^{-6} to 5×10^{-3} M existence of aggregated species in pure water. Upon increasing the concentration, hypochromic shift of the absorption bands at 500 and 535 nm for each of **(O)-L-** and **(O)-D-Ala-PBI**, and at 503 and 538 nm for each of **(O)-L-** and **(O)-D-Phe-PBI** occurred (Figure 1b,c and S1b,c). In contrast to the PBIs of the **(N)**-series, the dioxa derivatives form more extended aggregates

and hence tend slowly to precipitate in pure water due to decrease of positive charges and incorporation of more hydrophobic oxygen atoms in the side chains. However, the positions of the absorption maxima and the spectra shapes suggest that similar H-type aggregates as for the **(N)**-series are formed. On the other hand, the concentration-dependent UV/Vis spectra of the **(O)**-series in DMSO revealed the presence of well dissolved monomeric species over the whole concentration range from 8×10^{-6} to 2×10^{-3} M (the absorption spectra of **(O)-L-Ala-PBI** are shown as representative example in Figure S1a). Thus, stock solutions of **(O)**-series PBIs were prepared in DMSO for the studies with DNA/RNA (see next Section).

For the investigation with DNA/RNA, it is also of importance to know whether the addition of salts has any influence on the ionic self-assembly behavior of the newly synthesized homochiral PBIs, since such experiments are performed in buffer solutions of defined ionic strength. Thus, aggregation behavior of these PBIs at different salt concentrations has been studied by UV/Vis spectroscopy by adding up to 0.1 M of 1 M $NaCl_{aq}$ solution to the water solution of a particular PBI. Upon addition of increasing amounts of NaCl solution (from 0 to 0.1 M) to the aqueous solution of **(N)-L-** ($c = 5 \times 10^{-6}$ M) or **(N)-D-Phe-PBI** (1.25×10^{-5} M) the monomeric bands at 537 and 500 nm (for each of the enantiomers) gradually decreased (Figure S2a,b). Similar ionic strength induced aggregation was previously observed for **(N)-L-** and **(N)-D-Ala-PBI**.[16] As mentioned above, due to higher aggregation propensity of the less charged dioxa derivatives **(O)-L-** and **(O)-D-Ala-PBI** and **(O)-L-** and **(O)-**
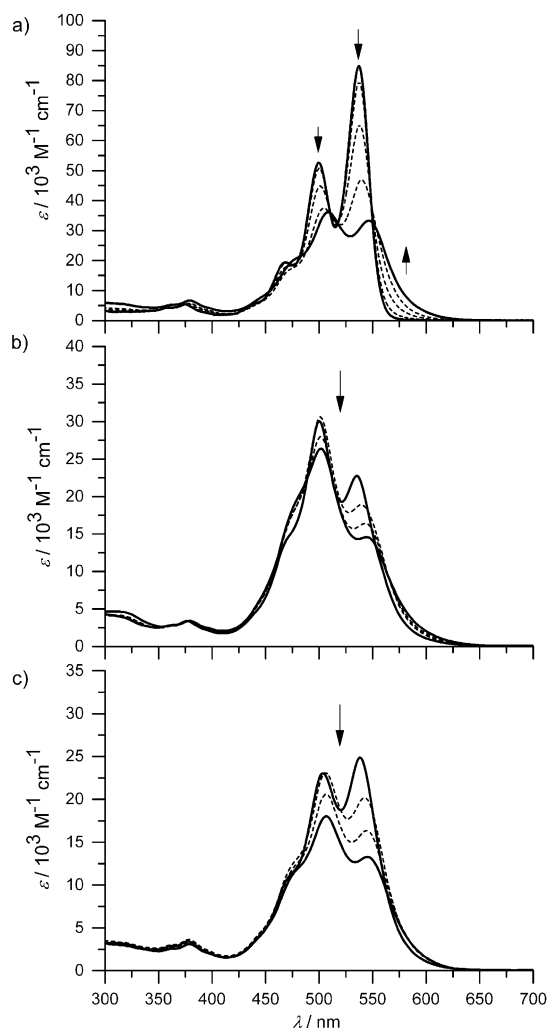
Figure 1. Concentration-dependent UV/Vis spectra ($c = 5 \times 10^{-6}$ to 5×10^{-3} M) of a) **(N)**-ʟ-**Phe-PBI**, b) **(O)**-ʟ-**Ala-PBI** and c) **(O)**-ʟ-**Phe-PBI** in water. Arrows indicate the spectral changes upon increasing concentration.

ᴅ-**Phe-PBI**, aggregate bands of these PBIs are evident even at a low concentration of $c = 5 \times 10^{-6}$ M (for each) in water. The addition of NaCl solution (from 0 to 0.1 M) to aqueous solutions of these PBIs at this concentration provoked hypochromic shift and changes in relative intensity for the vibronic excitonically coupled absorption bands, clearly indicating growth of larger PBI aggregates (Figure S2c–f).

Thermal denaturation of ds-DNA in the presence of PBIs

We have explored the interaction of homochiral PBIs **(N)**-ʟ- and **(N)**-ᴅ-**Ala-PBI**, **(N)**-ʟ- and **(N)**-ᴅ-**Phe-PBI**, and their dioxa analogues **(O)**-ʟ- and **(O)**-ᴅ-**Ala-PBI**, and **(O)**-ʟ- and **(O)**-ᴅ-**Phe-PBI** with ds-polynucleotides by the commonly used DNA thermal denaturation method. By this method the differences in melting temperatures (ΔT_m) of free ds-polynucleotides and their complexes with ligands (small molecules) are determined by UV/Vis spectroscopy, which provide valuable information on non-covalent interactions between DNA and small molecules.[22] Based on the results of UV/Vis absorption studies discussed before, for the DNA experiments stock solutions of

spermine-containing PBI derivatives (**(N)**-series) were prepared in water ($c \sim 10^{-4}$ M, no salt nor buffer added), while those of dioxa analogues (**(O)**-series) in DMSO ($c \sim 10^{-4}$ M). By using DMSO stock solutions, time- and temperature-stable solutions of **(O)**-series PBIs in cacodylate buffer (pH 7) could be obtained in which the content of DMSO never exceeded 1 vol %. Afterwards, mixtures of a chosen polynucleotide and one of the present PBIs were prepared by adding stock solution of the respective PBI to dissolved polynucleotide in cacodylate buffer (pH 7) reaching a particular concentration ratio $r = [c(\text{PBI})]/[c(\text{polynucleotide})]$.

Since in many cases precipitation was observed at $r > 0.1$, thermal denaturation experiments were performed on solutions with $r = 0.025$–0.1. The thermal denaturation of poly(dA-dT)$_2$ with **(O)**-ʟ-**Ala-PBI** is shown as representative example in Figure 2. All of the present PBIs provoked an enhancement of the melting temperatures of the employed ds-polynucleotides even at these low concentration ratios. At $r = 0.05$–0.1, for the complexes of spermine-containing PBI derivatives **(N)**-ʟ-and **(N)**-ᴅ-**Ala-PBI** and **(N)**-ʟ- and **(N)**-ᴅ-**Phe-PBI** with all of the applied ds-polynucleotides ΔT_m values between 7 and $> 35\,°C$ were observed, while the corresponding dioxa analogues showed considerably lower ΔT_m values between 3 and 30 °C (see Table 1). Obviously, due to larger number of positive charges (six each) the ΔT_m values of the **(N)**-series are higher than those observed for the **(O)**-series (two positive charges each).
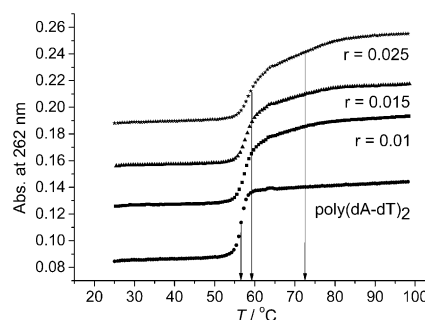
Figure 2. Thermal denaturation of poly(dA-dT)$_2$ upon addition of **(O)**-ʟ-**Ala-PBI** as a representative example; $r = [c(\text{compound})]/[c(\text{polynucleotide})] = 0.01$–0.025, at pH 7.0, buffer sodium cacodylate, $I = 0.05$ M.

Notably, at $r = 0.025$–0.05 most of the DNA denaturation experiments showed biphasic curves consisting of a transition of the PBI non-bound polynucleotide moiety (T_m similar to that of the respective free DNA/RNA) and a transition at the significantly higher T_m corresponding to the PBI/polynucleotide complex (see Figure 2 for an example). However, at $r = 0.05$–0.1 transitions of the free polynucleotides are either not present or observed in few cases with negligible intensity, which suggest complete saturation of PBI binding sites with the applied DNA and RNA at the ratio of $r = 0.1$. Only **(O)**-ʟ- and **(O)**-ᴅ-**Ala-PBI** with calf thymus (ct)-DNA and **(O)**-ᴅ-**Ala-PBI** with poly(dA-dT)$_2$ showed biphasic transitions even at $r = 0.1$, which is indicative of mixed binding modes.

Table 1. $\Delta T_m^{[a]}$ values [°C] of polynucleotides upon addition of PBIs to give different ratios $r^{[b]}$ at pH 7.0, buffer sodium cacodylate, $I = 0.05$ M.

PBI $r^{[b]}$	ct-DNA		poly A-poly U		poly dA-poly dT		poly(dA-dT)$_2$	
	0.05	0.1	0.05	0.1	0.05	0.1	0.05	0.1
(N)-Gly-PBI	17	>20[c]	16[d]	16	26	25	23	23
(N)-L-Ala-PBI[e]	>20[c]	>20[c]	15	–	15/>35[c,d]	–	13/25[d]	[c]
(N)-D-Ala-PBI[e]	17[c]	>17[c]	13/35[d]	>35[c]	16/>35[c,d]	>35[c]	17	[c]
(N)-L-Phe-PBI	16	>20[c]	33	33	17/28[c,d]	–	1/17[d]	18
(N)-D-Phe-PBI	7	8	33	31	15/>29[d]	15/>30[d]	13	14
(O)-L-Ala-PBI	4/>14[d]	6/>15[d]	10	10	–	4/10[d]	14	15
(O)-D-Ala-PBI	1/10[d]	3/11[d]	10	10	–	3/7[d]	4/10[d]	6/11[d]
(O)-L-Phe-PBI	3	5	8	9	–	29	–	5
(O)-D-Phe-PBI	3	4	9	10	–	30	7	7

[a] Error in $\Delta T_m \pm 0.5$ °C. [b] $r = [c(\text{compound})]/[c(\text{polynucleotide})]$. [c] T_m of complex >100 °C. [d] Biphasic thermal denaturation transitions. [e] Previous reported data are shown for comparison.[16]

natured, whereby excellent reproducibility between the first and second denaturation cycle was observed (representative examples are displayed in Figures S3, S4 in the Supporting Information), indicating the formation of the same type of complex.

Fluorimetric titrations of PBIs with DNA/RNA

We have then determined the binding constants for the complexes of present PBIs with different ds-polynucleotides by fluorimetric titration experiments. To avoid reabsorption, emission intensities were monitored above $\lambda > 590$ nm upon excitation at a wavelength of $\lambda_{ex} = 498$ nm. Processing of the fluorescence titration data by means of non-linear fit to Scatchard equation[25] provided binding constants $\log K_s$ for PBI/ds-polynucleotide complexes and pointed at saturation of dominant binding sites at r $[c(\text{PBI})/[c(\text{polynucleotide})]] = 0.1$. The binding constants obtained for the investigated PBIs with different polynucleotides are summarized in Table 2. The fluorescence titration spectra of the enantiomeric pair **(N)-L-** and **(N)-D-Phe-PBI** with poly(dG-dC)$_2$ are shown as representative examples in Figure S5, and those of the oxygen analogues **(O)-L-** and **(O)-D-Phe-PBI** with poly(dG-dC)$_2$ and poly(dA-dT)$_2$, respectively, in Figure S6.

The interaction of the ds-polynucleotides with **(N)**-series PBIs led to very high binding constants ($\log K_s = 9$–9.8). These values are significantly higher than those reported so far for non-covalently interacting molecules.[26] The addition of the employed

Since at $r = 0.1$ most of the denaturation curves are monophasic, and thus reveal the transition of the respective PBI/polynucleotide complex, a comparison of the melting temperature difference (ΔT_m) at this r value is most insightful. Spermine-containing achiral reference **(N)-Gly-PBI** showed with ds-DNA (ct-DNA, poly dA-poly dT and poly(dA-dT)$_2$) ΔT_m values above 20 °C and a lower ΔT_m value of 16 °C with RNA (poly A-poly U). The chiral spermine-functionalized analogues displayed with all of the used ds-polynucleotides ΔT_m values above 14 °C, in some cases even higher than 35 °C, with the exception of **(N)-D-Phe-PBI**. The latter displayed the weakest enhancement of the T_m value of 8 °C with ct-DNA in comparison to other spermine-substituted derivatives. This is most likely owing to the weak binding of **(N)-D-Phe-PBI** to the GC-base-pairs rich sequences of ct-DNA.

Oxygen-bearing PBIs (**(O)-L-** and **(O)-D-Ala-PBI**, and **(O)-L-** and **(O)-D-Phe-PBI**) exhibited larger variations in ΔT_m values at the ratio of $r = 0.1$ depending on the applied polynucleotides. **(O)-L-Ala-PBI** and **(O)-D-Ala-PBI** showed generally stronger DNA stabilization effect compared with that of the corresponding phenylalanine-substituted PBIs with ΔT_m values of higher than 10 °C. The phenylalanine-substituted PBIs **(O)-L-** and **(O)-D-Phe-PBI** revealed smaller ΔT_m values between 4 and 10 °C. This difference between the alanine- and the phenylalanine-substituted PBIs of the **(O)**-series reveals stronger influence of the steric hindrance at the chiral centers of the amino acids on the interaction of these PBIs with DNA compared to that of the **(N)**-series PBIs. The steric impact seems to be more pronounced when the amount of positive charges in the side chains is reduced. For the complexes of homonucleotide poly dA-poly dT with **(O)-L-** and **(O)-D-Phe-PBI** exceptionally high values around 30 °C were observed which is remarkable for the quite narrow minor groove of this polynucleotide.[23] In the case of RNA no difference between the alanine- and the phenylalanine-substituted PBIs could be observed since for both systems an average ΔT_m value of around 9 °C was determined. Apparently, the wide RNA groove provides sufficient space thus the steric hindrance does not play a significant role.[24] Moreover, several DNA/PBI complexes were submitted to slow cooling to room temperature after thermal denaturation to allow re-annelation of the complexes and again thermally de-

Table 2. Binding constants $\log K_s^{[a]}$ determined from the fluorescence titration data of PBIs with ds-polynucleotides at pH 7.0, buffer sodium cacodylate, $I = 0.05$ M.

	poly(dA-dT)$_2$ $\log K_s$/Int.[b]	poly(dG-dC)$_2$ $\log K_s$/Int.[b]	poly dA-poly dT $\log K_s$/Int.[b]	poly A-poly U $\log K_s$/Int.[b]
(N)-Gly-PBI	8–9[d]	8–9[d]	8–9[d]	8–9[d]
(N)-L-Ala-PBI[c]	9.7/0	>9[e]/0	9.4/0	9.8/0
(N)-D-Ala-PBI[c]	9.6/0	9.5/0	9.5/0	9.5/0
(N)-L-Phe-PBI	9.5/0	>9[e]/0	9.7/0	9.4/0
(N)-D-Phe-PBI	9.4/0	9.7/0	9.6/0	9.2/0
(O)-L-Ala-PBI	7.9/0.13	6.9/0.07	7.5/0.3	6.9/0.27
(O)-D-Ala-PBI	7.3/0.15	7.2/0.22	7.6/0.3	7.5/0.4
(O)-L-Phe-PBI	6.8/0.15	6.5/0.23	6.9/0.42	7.6/0.39
(O)-D-Phe-PBI	6.8/0.46	6.8/0.25	6.7/0.37	7.5/0.19

[a] The best Scatchard fit was obtained for ratio n ([bound PBI]/[polynucleotide]) = 0.2–0.1, and for easier comparison all binding constants were re-calculated for the fixed ratio n ([bound PBI]/[polynucleotide]) = 0.1. [b] Int. = Relative fluorescence emission intensity at the end of titration. [c] Previously reported data added for comparison.[16] [d] Oscillation of **(N)-Gly-PBI** fluorescence during titration with DNA/RNA allowed only estimation of the affinity within the given order of magnitude. [e] Almost linear emission quenching till Int. = 0 (reached at $r[c(\text{PBI})]/[c(\text{polynucleotide})]] = 0.1$), which allowed only an estimation by Scatchard fit.

polynucleotides to highly charged spermine-functionalized derivatives ((N)-L- and (N)-D-Ala-PBI, (N)-L- and (N)-D-Phe-PBI), respectively, completely quenched their fluorescence at the saturation regime (Int. = 0, see Table 2).

This emission quenching can be attributed to the formation of non-fluorescent H-type PBI aggregates[15b, 27] and their binding to polynucleotides.[28] In contrast to (N)-series PBIs, the dioxa analogues (O)-L- and (O)-D-Ala-PBI, and (O)-L- and (O)-D-Phe-PBI remained even upon saturation of DNA/RNA binding sites at the end of titration to some extent fluorescent (Int. = 0.07 to 0.46). Analysis of the binding parameters revealed that the dioxa analogues with two positive charges each bind more weakly to polynucleotides ($\log K_s = 6.5$ to 7.9) than the spermine derivatives with six positive charges ($\log K_s > 9$). Moreover, in contrast to the spermine derivatives, for dioxa analogues no trend between binding affinity and fluorescent properties of the formed PBI/polynucleotide complexes was observed. For example, the binding constants of (O)-L-Phe-PBI with poly(dA-dT)$_2$, poly(dG-dC)$_2$ and polydA-polydT are within the narrow range of 6.5–6.9, but the fluorescence intensities at saturation regime appreciably vary from 0.15 to 0.42 (see Table 2). Possible explanation for this observation could be delivered by fluorescence lifetime experiments. The single exponential fluorescence decay and the fluorescence lifetime of 4.5 ns were recorded for the (O)-L-Ala-PBI/ct-DNA complex under the same conditions as applied for fluorimetric titrations (see Figure S7). This could be explained by an equilibrium between the emissive PBI monomer and the non-emissive PBI aggregate within the ds-polynucleotides binding site. The huge excess of DNA/RNA used allows enough binding space within the grooves to accommodate such dimer-monomer equilibrium. The equilibrium is shifted towards strongly bound PBIs to ds-polynucleotides in the case of the (N)-series PBIs caused by additional interactions of the multiple positive charges of the side chains. Accordingly, these PBIs bind more strongly with ds-polynucleotides than their dioxa analogues.

CD spectroscopic studies of PBI/ds-polynucleotides complexes

To gain more insight into the DNA/RNA binding properties of chiral PBIs, we have performed circular dichroism (CD) spectroscopy studies by using a set of polynucleotides that possess specific minor groove features. Since achiral small molecules were reported to entail induced CD spectrum (ICD) upon binding to polynucleotides, providing useful information on DNA-binding modes,[29] we have first investigated the achiral glycine-bridged reference (N)-Gly-PBI. This inherently CD silent PBI, indeed, showed distinct ICD bands depending on the employed polynucleotide (Figure 3).

Addition of poly(dA-dT)$_2$ (4×10^{-5} M in sodium cacodylate buffer, pH 7) to this PBI ($r[c(PBI)]/[c(polynucleotide)] = 0.16$) provoked clear bisignate Cotton effect in the S_0–S_1 electronic transition region of PBI (> 400 nm) with maxima at 558 nm (-3.65 mdeg) and 498 nm (2.48 mdeg). Such bisignate CD signals are indicative of excitonic coupling of dyes which is only possible for dimers or larger aggregates with helical arrange-
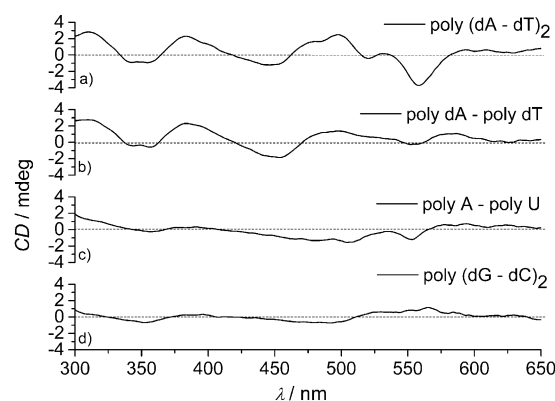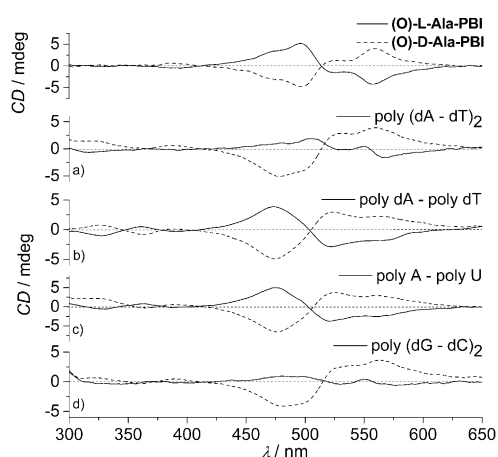

Figure 3. CD spectra of achiral reference (N)-Gly-PBI upon interaction with a) poly(dA-dT)$_2$, b) polydA-polydT, c) polyA-polyU and d) poly(dG-dC)$_2$ at pH 7.0 in sodium cacodylate buffer, $I = 0.05$ M; polynucleotide concentration: 4×10^{-5} M; $r[c(PBI)]/[c(polynucleotide)] = 0.16$.

ment. Likewise, for poly(dG-dC)$_2$ bisignate CD bands, but with opposite signs, at 564 nm (1.18 mdeg) and 492 nm (-0.72 mdeg) were observed. The signs of the CD signals with poly(dA-dT)$_2$ are similar to those previously reported for (N)-L-Ala-PBI with this polynucleotide,[16] which suggest the preference of the same type of PBI dimer aggregate in the groove of poly(dA-dT)$_2$ also for (N)-Gly-PBI. The guanine amino groups protruding into the GC-DNA minor groove may restrict the space to accommodate (N)-Gly-PBI dimer in minor groove of poly(dG-dC)$_2$, and thus less intensive bisignate CD signals are observed with this polynucleotide. The opposite signs of the respective signal with poly(dG-dC)$_2$, compared with those with poly(dA-dT)$_2$, obviously point at a different orientation of the anticipated PBI dimer in the groove. As shown in Figure 3, for the much narrower minor groove of polydA-polydT,[30] (N)-Gly-PBI exhibited similar CD spectral profile with maxima at 583 nm (1.03 mdeg) and 498 nm (1.37 mdeg) as observed for poly(dA-dT)$_2$ but with one significant difference, that is, the opposite sign of the long-wavelength band (> 550 nm), which might be due to the existence of more than one binding mode. Addition of (N)-Gly-PBI to A-U RNA resulted only in negative CD bands with maxima at 553 nm (-1.24 mdeg) and 506 nm (-1.58 mdeg). The absence of bisignate CD signals suggests the presence of single intercalated (N)-Gly-PBI molecule into RNA as a dominant binding mode.[7c, 31] Possible explanation for this might be that (N)-Gly-PBI does not have any significant steric hindrance due to the absence of a chiral substituent at the imide position, enabling intercalation into the minor groove of RNA that is wider than that of DNA.[32]

Next, we have investigated the CD spectroscopic profiles of chiral PBI derivatives in the presence of different polynucleotides that were also used for the achiral (N)-Gly-PBI. The CD spectroscopic features of alanine-functionalized derivatives (N)-L- and (N)-D-Ala-PBI with these polynucleotides have been reported previously.[16] Their hitherto unknown dioxa analogues (O)-L- and (O)-D-Ala-PBI, which contain significantly less positive charges (each two) compared with their (N)-counterparts (each six), have been investigated in a comparative manner to assess the impact of positive charges on DNA/RNA binding

properties that should be evident in CD spectra with different polynucleotides. The CD spectra of **(O)**-series PBIs are shown in Figure 4 and Figure S9 and, for the purpose of comparison, those of **(N)**-ʟ- and **(N)**-ᴅ-**Ala-PBI** in Figure S8.


Figure 4. CD spectra of **(O)**-ʟ- and **(O)**-ᴅ-**Ala-PBI** (note that CD spectra of **(O)**-ʟ- and **(O)**-ᴅ-**Ala-PBI** at 6×10^{-6} ᴍ in water without polynucleotides are depicted above) upon interaction with a) poly(dA-dT)$_2$, b) poly dA-poly dT, c) poly A-poly U and d) poly(dG-dC)$_2$ at pH 7.0 in sodium cacodylate buffer, $I = 0.05$ ᴍ; polynucleotide concentration: 4×10^{-5} ᴍ; $r[c(\text{PBI})]/[c(\text{polynucleotide})] = 0.15$; ʟ-configured PBI (solid line), ᴅ-configured PBI (dashed line).

The decrease of the positive charges in **(O)**-ʟ- and **(O)**-ᴅ-**Ala-PBI** resulted in higher aggregation tendency of these oxygen-bearing PBIs, compared to the respective **(N)**-analogues, leading to relatively strong bisignate CD signals at a concentration of 6×10^{-6} ᴍ in water in the absence of any polynucleotide. These bisignate CD signals originate from excitonic coupling of stacked PBI dyes and demonstrate the influence of the chiral substituents at the imide groups on the helicity of the columnar PBI π-stack.[33] The **(O)**-ʟ-**Ala-PBI** displayed CD signals at 557 nm (−4.2 mdeg) and 496 nm (5.2 mdeg) and the corresponding ᴅ-enantiomer at 558 nm (3.9 mdeg) and 496 nm (−4.6 mdeg). The two enantiomers share one isoelliptic point at 514 nm (Figure 4, top). CD spectra of different polynucleotides (4×10^{-5} ᴍ in 0.05 ᴍ sodium cacodylate buffer at pH 7) measured upon addition of varied amounts of each of these PBIs ($r[c(\text{PBI})]/[c(\text{polynucleotide})]$ up to 0.15) revealed emergence of excitonically coupled CD signals in the S$_0$–S$_1$ electronic transition region of PBI (>400 nm) with the strongest intensities at a ratio of $r = 0.15$ (see Figure S9). At this ratio, the CD spectra of the enantiomeric **(O)**-ʟ- and **(O)**-ᴅ-**Ala-PBI** showed for the applied polynucleotides distinctive spectral pattern (Figure 4). The CD signals of **(O)**-ᴅ-**Ala-PBI** with the various polynucleotides resemble those of PBI alone in water regarding both intensity and shape, which would mean that the PBI dimers formed in the grooves of DNA are similar to those formed in water in the absence of polynucleotides. The CD signals of the ʟ-enantiomer with all of the applied polynucleotides are of weaker intensity compared to those of the counter enantiomer, and PBI alone in water (Figure 4). Moreover, the CD signals of different shapes are observed for **(O)**-ʟ-**Ala-PBI**

with polynucleotides of diverse minor groove properties, indicating a different arrangement of the anticipated PBI dimers in the groove.

In contrast to **(O)**-ʟ- and **(O)**-ᴅ-**Ala-PBI**, phenylalanine derivatives of both **(O)**- and **(N)**-series display negligible CD signals at the concentration of 6×10^{-6} ᴍ in water in the absence of polynucleotides (Figure S10, S11 and Figure 5, top spectra). This result complies with our earlier finding that the bulky phenylalanine substituents prohibit the aggregation of the PBI dyes and that accordingly monomeric dyes are present at this low concentration (see Figure 1 and S1).
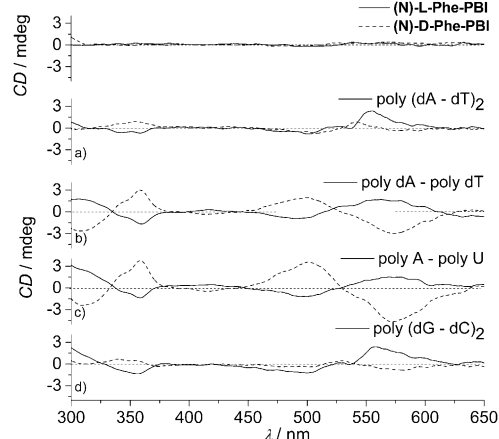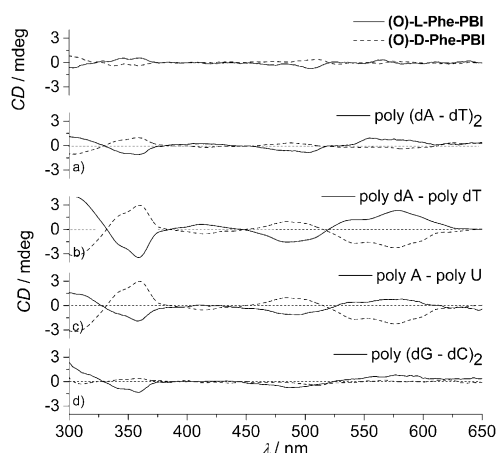

Figure 5. CD spectra of **(N)**-ʟ- and **(N)**-ᴅ-**Phe-PBI** upon interaction with a) poly(dA-dT)$_2$, b) poly dA-poly dT, c) poly A- poly U and d) poly(dG-dC)$_2$ at pH 7.0 in sodium cacodylate buffer, $I = 0.05$ ᴍ; polynucleotide concentration: 4×10^{-5} ᴍ; $r[c(\text{PBI})]/[c(\text{polynucleotide})] = 0.15$; ʟ-configured PBI (solid line), ᴅ-configured PBI (dashed line). CD spectra of **(N)**-ʟ- and **(N)**-ᴅ-**Phe-PBI** at 6×10^{-6} ᴍ in water alone are depicted at the top.

Interestingly, in the presence of polynucleotides these phenylalanine bearing PBIs showed, in most of the cases, CD bands in the region >400 nm that confirm the interaction between these PBIs and the chiral DNA scaffold. The CD spectral pattern of **(N)**-ʟ- and **(N)**-ᴅ-**Phe-PBI** at $r = 0.15$ revealed even bisignate Cotton effects with poly dA-poly dT and poly A-poly U at 570 and 490 nm which suggest the incorporation of PBI dimers in the minor grooves. The intensities of around 1.5/−1.0 mdeg for the ʟ-enantiomer and around −4.0/2.7 mdeg for the ᴅ-enantiomer (Figure 5) are, however, lower compared to those of the respective alanine derivatives **(N)**-ʟ- and **(N)**-ᴅ-**Ala-PBI** (Figure S8). This might be again due to the steric hindrance of the phenylalanine substituent. **(N)**-ᴅ-**Phe-PBI** exhibited rather negligible, small CD signals for poly(dA-dT)$_2$ and poly(dG-dC)$_2$, whereas for the ʟ-enantiomer comparatively strong bisignate CD signals at 550 nm (2.4 mdeg) and 500 nm (−0.98 mdeg) with these polynucleotides were observed. These configuration-dependent CD spectral properties are intriguing as they reveal that relatively small minor grooves of poly(dA-dT)$_2$ and poly(dG-dC)$_2$ can still accommodate dimers of ʟ-configured PBI, and obviously not those of ᴅ-configured one. Compared with **(O)**-ʟ- and **(O)**-ᴅ-**Ala-PBI**, the phenylalanine derivatives **(O)**-ʟ- and **(O)**-ᴅ-**Phe-PBI** showed less pro-

nounced CD signals revealing the impact of the steric hindrance of the benzyl substituent attached at the chiral centers of these PBIs.

The CD spectral pattern of **(O)**-L- and **(O)**-D-**Phe-PBI** showed bisignate Cotton effects with poly dA-poly dT and poly A-poly U at 575 nm and 490 nm with intensities of around $1.5/-1.3$ mdeg for the L-enantiomer and around $-2.3/1.0$ mdeg for the D-enantiomer (Figure 6).


Figure 6. CD spectra of and **(O)**-L- and **(O)**-D-**Phe-PBI** upon interaction with a) poly(dA-dT)$_2$, b) poly dA-poly dT, c) poly A- poly U and d) poly(dG-dC)$_2$ at pH 7.0 in sodium cacodylate buffer, $I = 0.05$ M; polynucleotide concentration: 4×10^{-5} M; $r[c(\text{PBI})]/[c(\text{polynucleotide})] = 0.15$; L-configured PBI (solid line), D-configured PBI (dashed line). CD spectra of **(O)**-L- and **(O)**-D-**Phe-PBI** alone at a concentration of 6×10^{-6} M in water are depicted at the top.

(O)-L-**Phe-PBI** exhibited with poly(dA-dT)$_2$ and poly(dG-dC)$_2$ CD signals at 560 nm (0.90 mdeg) and 490 nm (0.80 mdeg), while the CD signals of the respective D-enantiomer are nearly negligible. These results indicate again high preference for one enantiomer (in this case L-enantiomer) in the minor groove of these polynucleotides. Moreover, upon thermal denaturation followed by slow cooling, the ICD band pattern was fully reconstituted (a representative example is shown in Figure S12), pointing at the consistency of the complex formed. Such enantioselective sensing of polynucleotide secondary structure with small molecules has rarely been reported, thus homochiral PBIs are of high interest for potential application in DNA/RNA sensing.

Molecular modeling

Our spectroscopic results have clearly shown that PBI dimers are formed in the groove of ds-DNA/RNA. For the visualization of the PBI dimer/polynucleotide complexes and to corroborate our spectroscopic results, we have performed molecular modeling studies. For these studies, we have chosen **(O)**-L-**Ala-PBI** as a representative example for PBI derivatives and ds-polynucleotides poly(dA-dT)$_2$ (Figure 7a) and poly(dG-dC)$_2$ (Figure 7b) with minor grooves of different widths and performed 10 ns molecular modelling simulations.
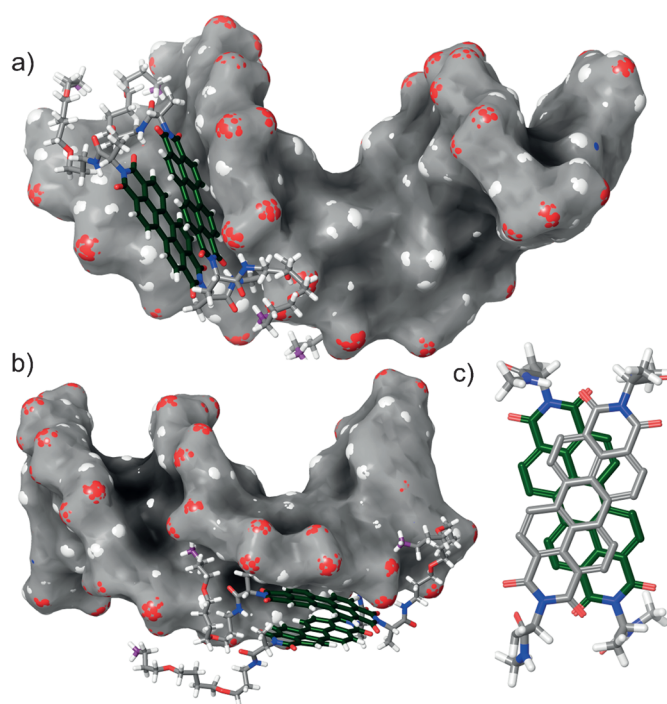
Figure 7. Modeled structure of the a) **(O)**-L-**Ala-PBI** dimer/poly(dA-dT)$_2$ complex and b) **(O)**-L-**Ala-PBI** dimer/poly(dG-dC)$_2$ complex obtained after 10 ns simulations in water at room temperature, reflecting the orientation and the arrangement of the PBI dimer aggregate within the minor groove of the ds-polynucleotide. c) Modeled structure of the free **(O)**-L-**Ala-PBI** dimer with left-handed (*M*-configuration) helicity in water (*OPLS 2001**).

The positions of positively charged aliphatic substituents are expected to change between various interaction contacts (e.g., with phosphate backbone) in thermodynamic equilibrium due to their own flexibility as well as the dynamic nature of DNA, while the main aim of modelling study is to give insight into the orientation of PBI dimer within the DNA binding site as well as orientation between two PBI molecules within the dimer. This will allow not only visual perception the structure of the complex formed, but also suggest possible inter- and intramolecular interactions of PBI within the binding site (minor groove), which should be instructive for the design of new compounds.

During 10 ns simulations (see Supporting Information for details) of the **(O)**-L-**Ala-PBI** dimer/poly(dA-dT)$_2$ complex at room temperature, the PBI molecules nicely accommodated into the minor grove of the polynucleotide. In this orientation the **(O)**-L-**Ala-PBI** dimer aggregate is bound to the poly(dA-dT)$_2$ by four strong hydrogen bonds formed between the terminal protonated amine groups and the phosphate groups of the DNA backbone. This model of the PBI/DNA complex illustrate that, although the PBI dimer aggregate retained in the left-handed (*M*) helical configuration, the mutual position of the two PBI molecules is not perfectly centered as depicted in the molecular model of the free **(O)**-L-**Ala-PBI** dimer aggregate (Figure 7c). This difference in molecular structure of free PBI dimer and PBI/DNA complex explains the differences in the CD signal patterns observed for the complex of **(O)**-L-**Ala-PBI** with poly-

nucleotides and free **(O)**-ʟ-**Ala-PBI** in water (see Figure 4). During the 10 ns simulations of the **(O)**-ʟ-**Ala-PBI** dimer/ poly(dG-dC)$_2$ complex the PBI dimer was not inserted deeply into the polynucleotide minor groove, as in the case of poly(dA-dT)$_2$. This is apparently due to the steric hindrance of guanine amino groups in poly(dG-dC)$_2$. Nevertheless, the complex was stabilized by the hydrophobic interactions, two hydrogen bonds between the terminal protonated amine groups and the phosphate groups of the polynucleotide as well as one additional NH phosphate hydrogen bond (Figure 7 b).

Consequently, the dimer aggregate of **(O)**-ʟ-**Ala-PBI** is more exposed to the aqueous environment outside the DNA and is less penetrated into the minor groove. Thus, the PBI dimer gains orientation freedom along the DNA helical axis which enables various possible arrangements, leading to much weaker CD signals with respect to those of the **(O)**-ʟ-**Ala-PBI** dimer/ poly(dA-dT)$_2$ complex. The outcome of molecular modeling studies strongly supports our conclusion made on the basis of the results of UV/Vis, fluorescence and CD spectroscopic investigations that PBI dimer aggregates with pronounced excitonic coupling are formed in the minor groove of the ds-DNA.

Conclusion

In summary, we have synthesized three new enantiomeric pairs of amino acid functionalized amphiphilic perylene bisimide dyes. Our in-depth studies with this broad series of homochiral ionic PBIs possessing varying number of positive charges, steric hindrance and the chiral information revealed convincing structure–property relationships for the interaction of PBI dyes with ds-polynucleotides. Thermal denaturation experiments, fluorimetric titrations and CD measurements confirmed the formation of stable PBI/polynucleotide complexes for the investigated PBIs. The spermine-containing PBIs having six positive charges each exhibited stronger DNA stabilization effect and higher binding constants compared with their dioxa analogues having only two positive charges each, thereby the latter PBIs showed more specific differences depending on their structural features. The CD spectroscopic studies revealed marked differences in ds-DNA/RNA binding properties of PBIs depending on the steric hindrance of the amino acids attached at the imide positions of the PBIs and their configuration, on the one hand, and groove properties of the employed ds-DNA/RNA, on the other hand. The formation of the excitonically coupled PBI dimer aggregates in the minor groove of ds-DNA and the major groove of ds-RNA can be implied from the spectroscopic results, and the structures of PBI/polynucleotide complexes obtained from molecular modeling reinforce the spectroscopic results. Based on our highly interesting findings, we can conclude that the present homochiral PBI dyes should be relevant for the enantioselective sensing of DNA/RNA secondary structures.

Experimental Section

Experimental details are presented in the Supporting Information.

[1] R. B. Silverman, *The organic chemistry of drug design and drug action*, 2nd ed., Elsevier Academic Press, Amsterdam, **2004**.
[2] E. Trinquet, G. Mathis, *Mol. BioSyst.* **2006**, *2*, 380 – 387.
[3] M. Demeunynck, C. Bailly, W. D. Wilson, Small molecule DNA and RNA binders: from synthesis to nucleic acid complexes, Wiley-VCH, Weinheim, **2003**.
[4] B. Willis, D. P. Arya, *Biochemistry* **2010**, *49*, 452 – 469.
[5] L. Xue, N. Ranjan, D. P. Arya, *Biochemistry* **2011**, *50*, 2838 – 2849.
[6] A. Ruiz-Carretero, P. G. A. Janssen, A. Kaeser, A. P. H. J. Schenning, *Chem. Commun.* **2011**, *47*, 4340 – 4347.
[7] a) S. M. Biner, D. Kummer, V. L. Malinovskii, R. Häner, *Org. Biomol. Chem.* **2011**, *9*, 2628 – 2633; b) M. Hariharan, Y. Zheng, H. Long, T. A. Zeidan, G. C. Schatz, J. Vura-Weis, M. R. Wasielewski, X. B. Zuo, D. M. Tiede, F. D. Lewis, *J. Am. Chem. Soc.* **2009**, *131*, 5920 – 5929; c) C. Wagner, H.-A. Wagenknecht, *Org. Lett.* **2006**, *8*, 4191 – 4194.
[8] M. Franceschin, *Eur. J. Org. Chem.* **2009**, 2225 – 2238.
[9] L. Rossetti, G. D'Isa, C. Mauriello, M. Varra, P. De Santis, L. Mayol, M. Savino, *Biophys. Chem.* **2007**, *129*, 70 – 81.
[10] a) J. T. Kern, P. W. Thomas, S. M. Kerwin, *Biochemistry* **2002**, *41*, 11379 – 11389; b) W. Tuntiwechapikul, T. Taka, M. Béthencourt, L. Makonkawkeyoon, T. R. Lee, *Bioorg. Med. Chem. Lett.* **2006**, *16*, 4120 – 4126; c) E. Micheli, C. M. Lombardo, D. D'Ambrosio, M. Franceschin, S. Neidle, M. Savino, *Bioorg. Med. Chem. Lett.* **2009**, *19*, 3903 – 3908.
[11] D. Baumstark, H. A. Wagenknecht, *Chem. Eur. J.* **2008**, *14*, 6640 – 6645.
[12] a) L.-M. Tumir, I. Crnolatac, T. Deligeorgiev, A. Vasilev, S. Kaloyanova, M. Grabar Branilović, S. Tomić, I. Piantanida, *Chem. Eur. J.* **2012**, *18*, 3859 – 3864; b) K. Klemm, M. Radić Stojković, G. Horvat, V. Tomišić, I. Piantanida, C. Schmuck, *Chem. Eur. J.* **2012**, *18*, 1352 – 1363; c) M. Radić Stojković, S. Miljanić, K. Mišković, L. Glavaš-Obrovac, I. Piantanida, *Mol. BioSyst.* **2011**, *7*, 1753 – 1765.
[13] a) T. Seki, X. Lin, S. Yagai, *Asian J. Org. Chem.* **2013**, *2*, 708 – 724; b) X. Zhan, A. Facchetti, S. Barlow, T. J. Marks, M. A. Ratner, M. R. Wasielewski, S. R. Marder, *Adv. Mater.* **2011**, *23*, 268 – 284; c) F. Würthner, M. Stolte, *Chem. Commun.* **2011**, *47*, 5109 – 5115; d) F. Würthner, *Chem. Commun.* **2004**, 1564 – 1579.
[14] a) C. D. Schmidt, C. Böttcher, A. Hirsch, *Eur. J. Org. Chem.* **2007**, 5497 – 5505; b) C. D. Schmidt, C. Böttcher, A. Hirsch, *Eur. J. Org. Chem.* **2009**, 5337 – 5349; c) E. Krieg, E. Shirman, H. Weissman, E. Shimoni, S. G. Wolf, I. Pinkas, B. Rybtchinski, *J. Am. Chem. Soc.* **2009**, *131*, 14365 – 14373; d) D. Franke, M. Vos, M. Antonietti, N. A. J. M. Sommerdijk, C. F. J. Faul, *Chem. Mater.* **2006**, *18*, 1839 – 1847; e) Y. Huang, Y. Yan, B. M. Smarsly, Z. Wei, C. F. J. Faul, *J. Mater. Chem.* **2009**, *19*, 2356 – 2362; f) D. Görl, X. Zhang, F. Würthner, *Angew. Chem. Int. Ed.* **2012**, *51*, 6328 – 6348; *Angew. Chem.* **2012**, *124*, 6434 – 6455.
[15] a) M. Franceschin, A. Rizzo, V. Casagrande, E. Salvati, A. Alvino, A. Altieri, A. Ciammaichella, S. Iachettini, C. Leonetti, G. Ortaggi, M. Porru, A. Bianco, A. Biroccio, *ChemMedChem* **2012**, *7*, 2144 – 2154; b) S. Rehm, V. Stepanenko, X. Zhang, T. H. Rehm, F. Würthner, *Chem. Eur. J.* **2010**, *16*, 3372 – 3382; c) B. Roy, T. Noguchi, D. Yoshihara, Y. Tsuchiya, A. Dawn, S. Shinkai, *Org. Biomol. Chem.* **2014**, *12*, 561 – 565.
[16] T. H. Rehm, M. Radić Stojković, S. Rehm, M. Škugor, I. Piantanida, F. Würthner, *Chem. Sci.* **2012**, *3*, 3393 – 3397.
[17] V. Casagrande, A. Alvino, A. Bianco, G. Ortaggi, M. Franceschin, *J. Mass Spectrom.* **2009**, *44*, 530 – 540.

[18] Y. Xu, S. Leng, C. Xue, R. Sun, J. Pan, J. Ford, S. Jin, *Angew. Chem. Int. Ed.* **2007**, *46*, 3896–3899; *Angew. Chem.* **2007**, *119*, 3970–3973.

[19] A. J. Geall, I. S. Blagbrough, *Tetrahedron* **2000**, *56*, 2449–2460.

[20] a) S. Fixon-Owoo, F. Levasseur, K. Williams, T. N. Sabado, M. Lowe, M. Klose, A. Joffre Mercier, P. Fields, J. Atkinson, *Phytochemistry* **2003**, *63*, 315–334; b) P. Wellendorph, J. W. Jaroszewski, S. H. Hansen, H. Franzyk, *Eur. J. Med. Chem.* **2003**, *38*, 117–122.

[21] Z. Chen, B. Fimmel, F. Würthner, *Org. Biomol. Chem.* **2012**, *10*, 5845–5855.

[22] M. Nakamura, Y. Shimomura, Y. Ohtoshi, K. Sasa, H. Hayashi, H. Nakano, K. Yamana, *Org. Biomol. Chem.* **2007**, *5*, 1945–1951.

[23] C. R. Cantor, P. R. Schimmel, *The behavior of biological macromolecules*, W. H. Freeman, San Francisco, **1980**.

[24] S. Neidle, in *Principles of Nucleic Acid Structure*, Academic Press, New York, **2008**, pp. 204–248.

[25] a) G. Scatchard, *Ann. N. Y. Acad. Sci.* **1949**, *51*, 660–672; b) J. D. McGhee, P. H. v. Hippel, *J. Mol. Biol.* **1976**, *103*, 679.

[26] L. Strekowski, B. Wilson, *Mutat. Res.* **2007**, *623*, 3–13.

[27] T. Heek, C. Fasting, C. Rest, X. Zhang, F. Würthner, R. Haag, *Chem. Commun.* **2010**, *46*, 1884–1886.

[28] a) N. Rahe, C. Rinn, T. Carell, *Chem. Commun.* **2003**, 2120–2121; b) P. P. Neelakandan, Z. Pan, M. Hariharan, Y. Zheng, H. Weissman, B. Rybtchinski, F. D. Lewis, *J. Am. Chem. Soc.* **2010**, *132*, 15808–15813; c) R. Varghese, H.-A. Wagenknecht, *Chem. Commun.* **2009**, 2615–2624; d) D. Baumstark, H.-A. Wagenknecht, *Angew. Chem. Int. Ed.* **2008**, *47*, 2612–2614; *Angew. Chem.* **2008**, *120*, 2652–2654.

[29] A. Rodger, B. Norden, *Circular Dichroism and Linear Dichroism*, Oxford University Press, New York, **1997**; N. Harada, K. Nakanishi, *Acc. Chem. Res.* **1972**, *5*, 257–263.

[30] W. D. Wilson, Y. H. Wang, C. R. Krishnamoorthy, J. C. Smith, *Biochemistry* **1985**, *24*, 3991–3999.

[31] T. Biver, *Appl. Spectrosc. Rev.* **2012**, *47*, 272–325.

[32] W. D. Wilson, L. Ratmeyer, M. Zhao, L. Strekowski, D. Boykin, *Biochemistry* **1993**, *32*, 4098–4104.

[33] V. Dehm, Z. Chen, U. Baumeister, P. Prins, L. D. A. Siebbeles, F. Würthner, *Org. Lett.* **2007**, *9*, 1085–1088.